

# Analysis of Massive MIMO and Base Station Cooperation in an Indoor Scenario

Stefan Dierks, Gerhard Kramer, *Fellow, IEEE*, Berthold Panzner, *Senior Member, IEEE*, and Wolfgang Zirwas,

**Abstract**—The performance of centralized and distributed massive MIMO deployments are analyzed for indoor office scenarios. The distributed deployments use one of the following precoding methods: (1) local precoding with local channel state information (CSI) to the user equipments (UEs) that it serves; (2) large-scale MIMO with local CSI to all UEs in the network; (3) network MIMO with global CSI. For the distributed deployments (2) and (3), it is shown that using twice as many base station antennas as data streams provides many of the massive MIMO benefits in terms of spectral efficiency and fairness. This is in contrast to the centralized deployment and the distributed deployment (1) where more antennas are needed. Two of the main conclusions are that distributing base stations helps to overcome wall penetration loss; however, a backhaul is required to mitigate inter-cell interference. The effect of estimation errors on the performance is also quantified.

## I. INTRODUCTION

ONE goal of new mobile radio communication standards, e.g., 5th generation mobile networks (5G), is to increase the spectral efficiency (SE) per unit area or volume. For example, the METIS (Mobile and wireless communications Enablers for the Twenty-twenty Information Society) project [1] defines target traffic volume densities for different scenarios. One way to increase SE is by using multiple-input multiple-output (MIMO) schemes. MIMO allows one node to transmit several streams to one or more user equipments (UEs) using spatial degrees-of-freedom.

*Massive MIMO* refers to a “vast” over-provisioning of base station (BS) antennas as compared to the number of served single antenna UEs [2]. Massive MIMO is also known as “Very Large MIMO”, “Hyper MIMO”, “Full Dimension MIMO”, “Large-Scale Antenna Systems”, or “ARGOS” [3]. However, the term massive MIMO is not clearly defined. Massive MIMO may refer to any MIMO configuration beyond the largest MIMO mode in the current LTE standard (at present 8x8), e.g., 100 antennas or more [4], or it may simply refer to a “large” number of antennas at the BSs. A more precise definition of massive MIMO is based on the ratio  $M/K$  of serving BS antennas  $M$  to the number  $K$  of active UEs. However, the ratio  $M/K$  for which one can speak of massive MIMO depends on the performance metric, the scenario, etc. [5].

Massive MIMO claims several advantages over conventional MIMO [3]:

S. Dierks and G. Kramer are with the Chair for Communications Engineering, Technical University of Munich, Germany, e-mail: {stefan.dierks, gerhard.kramer}@tum.de

B. Panzner and W. Zirwas are with Nokia Networks, Munich, Germany, email: {berthold.panzner, wolfgang.zirwas}@nokia.com

- *Massive MIMO increases capacity by 10 times or more and simultaneously increases energy efficiency.* The transmit signals are directed precisely to the UEs through precoding which reduces interference. Each additional antenna increases the precoding degrees-of-freedom assuming no mutual coupling and a sufficiently complex propagation environment [4].
- *Inexpensive, low-power components suffice.* A large number of BS antennas makes the system robust against noise, fading and hardware impairments or even failure of antenna elements. This allows simpler transmitters and receivers at the BS, e.g., few or one bit quantization, hybrid digital-analog precoding, and constant envelope precoding [5].
- *Precoding simplifies.* Simple linear precoding has a vanishing gap to optimal precoding [2], [4], [5]. For instance, the performance gap between linear zero-forcing beamforming (ZFBB) [6] and the optimal, non-linear dirty paper coding (DPC) [7] vanishes with an increasing number of BS antennas. Maximum ratio transmission (MRT) is also asymptotically optimal as the number of BS antennas increases, but for a smaller number of BS antennas MRT performs well only in the low signal-to-noise ratio (SNR) regime [4].
- *The multiple-access layer simplifies.* The channel hardens by the law of large numbers [3], [4]. This means that all subcarriers experience similar small-scale fading and the UE channel vectors become orthogonal. Hence scheduling does not improve performance because all UEs can be active on all subcarriers. Only power control is needed to distribute the power depending on the slowly varying large-scale fading [5].
- *The latency is reduced.* Since all UEs can always be active, UEs need not wait for good fading conditions.
- *Massive MIMO is robust to jamming and interference.* The surplus of precoding degrees-of-freedom can be used to cancel interference or jamming.

Most massive MIMO studies consider wide area outdoor scenarios [2], [3], [5]. However, most mobile traffic is generated by indoor users [8]. We analyze the performance of different BS deployments with different levels of cooperation for the 3rd Generation Partnership Project (3GPP) indoor office scenario [9]. Our approach is as follows. We fix the number of active, single antenna UEs and sweep the ratio of total number of BS antennas to the number of active UEs from one to ten. We find that a ratio of twice as many BS antennas provides most of the massive MIMO benefits. We further find

that this ratio is a good tradeoff between number of antennas versus SE. We present suboptimal transmission schemes that approach a capacity upper bound. We analyze fairness using Jain's index [10].

We further compare massive MIMO to distributed MIMO. The motivation is that placing a single massive MIMO BS at the center of a building causes UEs to experience large path loss and high wall penetration loss. We compare this deployment to distributed BSs. We find that distributed indoor BSs with cooperation achieve a substantial performance gain at the cost of a backhaul connection, while the gain achieved with cooperation between outdoor BSs and a single indoor BS is smaller. With increasing capability of the backhaul, the cooperation level can be increased which allows to achieve the same performance with fewer BS antennas.

Finally, we quantify the performance loss due to channel estimation error. Like in conventional MIMO, channel state information (CSI) is required to enable precoding. Acquiring CSI might be more difficult in massive MIMO due to the many antennas. Frequency division duplex (FDD) requires a pilot sequence for each BS antenna, while time division duplex (TDD) suffers from pilot contamination [2].

Our results help guide design choices for future mobile radio communication systems, e.g., Long Term Evolution-Advanced (LTE-Advanced) and 5G. We presented preliminary results in [11], [12], [13], and we add the following results.

- Instead of using water-filling to allocate power, we use mercury/water-filling, which is optimal for finite modulation alphabets [14].
- We analyze two additional deployments (the *two indoor BSs* deployment and the *fourty indoor BSs* deployment).
- We add large-scale MIMO (LS-MIMO) as an example of an interference coordination scheme.
- We analyze fairness for Gaussian modulation.

We denote vectors with bold lower case letters, and matrices with bold upper case letters. The transpose of  $\mathbf{X}$  is  $\mathbf{X}^T$  and the complex conjugate transpose is  $\mathbf{X}^H$ . The Euclidean norm of  $\mathbf{x}$  is  $\|\mathbf{x}\|_2$ , and the Frobenius norm of  $\mathbf{X}$  is  $\|\mathbf{X}\|_F$ . We denote a diagonal matrix having diagonal entries  $\mathbf{x}$  as  $\text{diag}(\mathbf{x})$ .

## II. SYSTEM MODEL

Consider the downlink in the 3GPP "A1 - Indoor Office" scenario in the Wireless World Initiative New Radio II (WINNER II) deliverable [15], see Fig. 1. The UEs are served by BSs located inside and outside the building, and we describe the BS deployments in Section IV-A. We consider  $K$  single antenna UEs and orthogonal frequency-division multiplexing (OFDM). For each subcarrier we obtain a broadcast channel (BC). The received signal of the  $k$ -th UE for one subcarrier is

$$y_k = \mathbf{h}_k^H \mathbf{x} + z_k \quad k \in \{1, \dots, K\} \quad (1)$$

where  $\mathbf{h}_k^H = [\mathbf{h}_{k,1}^H, \dots, \mathbf{h}_{k,N_{\text{BS}}}^H]$  is the vector of channel coefficients from all  $N_{\text{BS}}$  BSs to the  $k$ -th UE. The  $i$ -th BS has  $M_i$  BS antennas with the channel coefficients  $\mathbf{h}_{k,i}^H$ . The dimension of  $\mathbf{h}_k^H$  is  $M = \sum_{i=1}^{N_{\text{BS}}} M_i$ . The transmit signal vectors are collected in  $\mathbf{x} = [\mathbf{x}_1^T, \dots, \mathbf{x}_{N_{\text{BS}}}^T]^T$  and the  $z_1, z_2, \dots, z_K$  are independent proper complex additive white Gaussian noise

(AWGN) random variables with variance  $\sigma_N^2$ . The received signals of all UEs  $\mathbf{y} = [y_1, \dots, y_K]^T$  for one subcarrier are collected in the vector

$$\mathbf{y} = \mathbf{H}^H \mathbf{x} + \mathbf{z} \quad (2)$$

where  $\mathbf{H}^H = [\mathbf{h}_1^H, \dots, \mathbf{h}_K^H]$  and  $\mathbf{z} = [z_1, \dots, z_K]^T$ .

For linear precoding the transmit signals vector  $\mathbf{x}$  is

$$\mathbf{x} = \mathbf{W} \mathbf{s} \quad (3)$$

where  $\mathbf{W} = [\mathbf{w}_1, \dots, \mathbf{w}_K]$  is the matrix of the precoding vectors and  $\mathbf{s} = [s_1, \dots, s_K]^T$  is the vector of transmit symbols. We assume that  $\mathbb{E}[|s_k|^2] = 1$  for  $k \in \{1, 2, \dots, K\}$ . We consider per-BS sum-power constraints

$$\sum_{f=1}^{N_{\text{SC}}} \mathbb{E} \left[ \|\mathbf{x}_i^{(f)}\|_2^2 \right] = \sum_{f=1}^{N_{\text{SC}}} \|\mathbf{W}_i^{(f)}\|_F^2 \leq P_i \quad \forall i \in \{1, \dots, N_{\text{BS}}\} \quad (4)$$

where  $N_{\text{SC}}$  is the number of subcarriers, and  $\mathbf{W}_i^{(f)}$  is the part of the precoding matrix that creates the transmit signals at the  $i$ -th BS  $\mathbf{x}_i^{(f)}$ . We often omit the subcarrier index if  $f$  is clear from the context.

## III. TRANSMISSION SCHEMES

Interference management is important for modern wireless communication standards like Long Term Evolution (LTE) [16], LTE-Advanced [17], and for future standards like 5G. A general framework and optimization algorithms for multi-cell scenarios with different levels of cooperation are presented in [18]. We are interested in transmission schemes with low complexity. For ease of notation we describe the principle for a single subcarrier and omit the subcarrier index.

### A. Local Precoding

*Local precoding* BSs determine the transmit signals and the scheduled UEs locally. They treat inter-cell interference as noise and thus interference limits reliable transmission in many scenarios. As a result, backhaul requirements are low and only local CSI is required.

Suppose each UE is served by the BS with the maximum average SNR. We use ZFBF [19] to mitigate intra-cell interference. The local precoding matrix at the  $i$ -th BS is

$$\mathbf{W}_i = \mathbf{H}_{i,i} \left( \mathbf{H}_{i,i}^H \mathbf{H}_{i,i} \right)^{-1} \text{diag}(\tilde{\mathbf{p}}_i)^{\frac{1}{2}} \quad (5)$$

where  $\mathbf{H}_{i,i}^H$  is the channel matrix from the  $i$ -th BS to its  $K_i$  UEs, and  $\tilde{\mathbf{p}}_i$  is the power allocation vector at the  $i$ -th BS. ZFBF requires that the  $i$ -th BS serves at most  $M_i$  UEs, i.e., we have  $K_i \leq M_i$ . If  $K_i > M_i$  then we use the low complexity scheduling algorithm from [20] to select  $M_i$  UEs. Note that the set of scheduled UEs may be different on each subcarrier. We use mercury/water-filling [14] at each BS to allocate power according to a per-BS power constraint.

## B. Large-Scale MIMO

Interference coordination has each BS estimate its channels to all UEs, and each BS exchange its CSI with the other BSs. The resulting global CSI lets us coordinate the transmissions of the BSs, e.g., by power allocation, precoding, and scheduling. In contrast, for local precoding each BS estimates only its channels to the UEs it serves. Interference coordination has each UE served by a single BS, and the backhaul requirements are modest because a signal-level synchronization of the BSs is not needed [21]. The UEs served by each BS are determined based on maximal SNR as for local precoding. The coordination can be accomplished at a central processor or locally at the BSs. The distributed, local coordination can be realized in a competitive (game theoretic) way or with the help of control messages over the backhaul. Note that to reduce the backhaul requirements some coordination schemes exchange little CSI, and some schemes exchange control messages instead.

The coordination schemes can be categorized as follows [21]:

- Coordinated scheduling (CS) has the scheduling and power allocation optimized jointly by all BSs.
- Coordinated beamforming (CB) has the precoding coordinated using available precoding degrees-of-freedom to reduce interference.
- The combination of CS and CB, which is called coordinated scheduling/coordinated beamforming (CS/CB), is more common than pure CB.
- For CS, CB, and CS/CB interference is treated as noise. Performance can improve if interference is detected at the UEs [21]. Interference detection can be supported by coding at the transmitter, e.g., by interference alignment.

We consider *large-scale MIMO (LS-MIMO)* [22] as an example of an interference coordination scheme. LS-MIMO is a linear CB scheme which does not exchange CSI or control messages over the backhaul. With sufficiently many antennas, each BS uses ZFBF to mitigate the interference created at all UEs and thereby creates parallel interference-free channels to the UEs it serves. This is feasible only if the number  $M_i$  of antennas at the  $i$ -th BS is at least as large as the total number of UEs, i.e., we have  $M_i \geq K$ . Hence LS-MIMO is feasible only if  $M \geq N_{\text{BS}}K$ .

Note that LS-MIMO can be made feasible by scheduling a subset of UEs. However, we analyze LS-MIMO only if  $M \geq N_{\text{BS}}K$ . We use ZFBF

$$\mathbf{W}_i = \mathbf{H}_i \left( \mathbf{H}_i^H \mathbf{H}_i \right)^{-1} \text{diag}(\tilde{\mathbf{p}}_i)^{\frac{1}{2}} \quad (6)$$

where  $\mathbf{H}_i^H$  is the channel matrix from the  $i$ -th BS to all UEs, and the power is allocated by mercury/water-filling [14]. Massive MIMO approaches the zero-forcing behavior of LS-MIMO with increasing  $M_i$  because channels to the UEs of the other BSs become orthogonal to the channels of the served UEs [22].

## C. Network MIMO

Network MIMO requires that the BSs are connected by a backhaul with low delay and high throughput, and that the

BSs are synchronized. The distributed BSs act as one BS with distributed antennas, and the downlink channel becomes a BC. In contrast to interference coordination, network MIMO may have interference enhance the signals at the UEs. Network MIMO can be realized by a central processor or by exchanging messages between the BSs.

For our *network MIMO* scheme, we assume a perfect backhaul with unlimited capacity and zero delay. We let all BSs act as a single BS with distributed antennas and apply ZFBF with per-BS power constraints. The classic multiple-access channel (MAC)-BC duality does not determine the optimal precoder for per-BS power constraints [21]. We use a low-complexity and suboptimal approach and determine for each subcarrier the ZFBF precoding matrix

$$\mathbf{W} = \mathbf{H} \left( \mathbf{H}^H \mathbf{H} \right)^{-1} \text{diag}(\tilde{\mathbf{p}})^{\frac{1}{2}} \quad (7)$$

where  $\tilde{\mathbf{p}}$  is the power allocation vector. We use mercury/water-filling [14] to allocate power according to a total power constraint

$$\sum_{f=1}^{N_{\text{sc}}} \mathbb{E} \left[ \left\| \mathbf{x}^{(f)} \right\|_2^2 \right] \leq \sum_{i=1}^{N_{\text{BS}}} P_i. \quad (8)$$

Next, we determine the transmit power at each BS and scale the precoding matrix  $\mathbf{W}$  so that the per-BS power constraint is satisfied at the BS with the maximal transmit power. Note that the other BSs could transmit with higher power. Hence this is a suboptimal approach, and better approaches can be found, e.g., see [23], [24].

Network MIMO helps to avoid rank deficient and poorly conditioned channel matrices which are caused by spatial correlations or by the “keyhole” effect [25]. Network MIMO is sometimes called “distributed MIMO”, “MIMO cooperation”, “coherently coordinated transmission”, “Joint Processing CoMP”, “Joint Transmission CoMP”, “C-RAN (Cloud-RAN)” or “p-cell” [26].

## IV. INDOOR SCENARIO

Figure 1 shows the layout of the indoor office scenario defined as “A1 - Indoor Office” in the WINNER II deliverable D.1.1.2 [15]. The UEs are located 1.5 m above the floor inside the building. We use the Quasi Deterministic Radio Channel Generator (QuaDRiGa) [27] to generate channel coefficients.

The indoor channels are generated according to the “A1 - Indoor Office” channel model parameters [15]. There are two parameter sets for line-of-sight (LOS) and for non line-of-sight (NLOS) conditions. For NLOS conditions a wall penetration loss is added, where the wall penetration loss is determined by counting the number of walls between each BS and UE beyond the first penetrated wall. When counting the number of walls, paths along the corridors are considered as alternatives to the direct path, which might penetrate more walls.

The outdoor-to-indoor channels are generated according to the “B4 - Outdoor to indoor” channel model parameters defined in Wireless World Initiative New Radio+ (WINNER+) deliverable D5.3 [28]. The outdoor BSs are below rooftop micro BSs. We assume a LOS path from the BS to the outside wall of the building. For each UE the pathloss is calculated

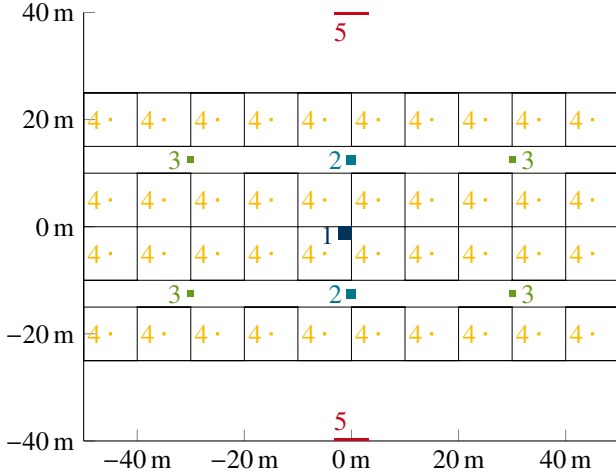


Fig. 1. Base station deployments in the indoor office scenario [15].

based on the path through the point on an outside wall nearest to the UE. The number of penetrated walls is determined as for the indoor BSs.

#### A. Base Station Deployments

We define six different BS deployments which are shown in Figure 1.

- *Single central BS* is a single BS with  $M$  antennas located in the corner of the room southwest of the center (“1” in Figure 1). This is a classical massive MIMO deployment.
- *Two indoor BSs* are two BSs with  $M/2$  antennas each. One BS is located in the center of each corridor (“2”).
- *Four indoor BSs* are four BSs with  $M/4$  antennas each. Two BSs are located in each corridor (“3”).
- *Forty indoor BSs* are forty BSs with  $M/40$  antennas each. One BS is located in the center of each room (“4”). This is similar to the deployment of p-cell [26].
- *Outdoor BSs* are two BSs with  $M/2$  antennas each. They are located 15 m north/south of the middle of the north/south outside wall (“5”).
- *Indoor-outdoor BSs* are three BSs with  $M/3$  antennas each. One BS is in the location of the *single central BS* deployment (“1”) while two are in the location of the *outdoor BSs* deployment (“5”).

Note that we need a sufficient backhaul (not shown in Figure 1) for all deployments except the *single central BS* deployment to permit network MIMO. Also note that the BSs are not necessarily optimally placed.

#### B. Antenna Array Configuration

The indoor BSs are rectangle arrays, while the outdoor BSs are uniform linear arrays (ULAs). The antennas are spaced at half wavelength distance  $\lambda_L/2$ . The rectangular arrays are mounted underneath the ceiling at a height of 3 m. We choose the side lengths of the rectangle such that  $\lceil \sqrt{M_i} \rceil$  antennas fit per row and column. Note that the last rows might not be fully occupied by antennas. The height of the outdoor BSs is 10 m and the antennas of the ULAs are located on a line parallel to

the long side of the building. We assume no mutual coupling between antennas. Unless otherwise stated, we assume ideal hardware, perfect synchronization, and perfect CSI of the complete network at all nodes.

## V. SIMULATION PARAMETERS

We fix the number of UEs to  $K = 24$  and compare the deployments with different performance measures for different numbers  $M$  of total BS antennas. We simulate 300 drops where one drop is a random placement of the 24 UEs within the office building. For each drop we generate 10 channel realizations. The wall penetration loss is 12 dB per wall. We use a bandwidth of 20 MHz around a carrier frequency of 2.1 GHz. The active bandwidth is 18 MHz and 1 MHz on each side of this bandwidth is a guard band. The subcarrier spacing is 15 kHz and we obtain 1200 subcarriers. In LTE, subcarriers are arranged in groups of 12 consecutive subcarriers which are called physical resource blocks (PRBs). Hence we obtain 100 PRBs. The channel conditions of the subcarriers of one PRB are usually very similar. The schedule, power allocation, and precoder are the same for all subcarriers of one PRB in LTE to save control signaling overhead. We save simulation time by simulating a single subcarrier per PRB and assuming that the same performance is achieved on the other subcarriers of the PRB.

Unless otherwise mentioned, we use 256 quadrature amplitude modulation (QAM) and mercury/water-filling to allocate power. The per-BS power in dBm at the  $i$ -th BS is constrained by

$$P_i = 26 \text{ dBm} - 10 \log_{10}(N_{\text{BS}}). \quad (9)$$

The maximal per-BS powers are such that the maximal sum power available to the BSs is 26 dBm. The variance of the AWGN at the UEs, i.e., the noise level, is  $\sigma_N^2 = -125.1$  dBm.

The simulation parameters are summarized in Table I. With these parameters, the per-UE SE  $S_k$  of the  $k$ -th UE without considering control signaling overhead is

$$S_k = \frac{12 \cdot \sum_{f=1}^{100} C \left( \text{SINR}_k^{(f)} \right) \cdot 14}{1 \text{ ms} \cdot 20 \text{ MHz}} \quad (10)$$

where 12 is the number of subcarriers per PRB, 100 is the number of PRBs, 14 is the number of OFDM blocks per subframe, 1 ms is the duration of one subframe and  $C \left( \text{SINR}_k^{(f)} \right)$  is the capacity at  $\text{SINR}_k^{(f)}$  of a memoryless channel with 256 QAM input and continuous output in bits [29]. The sum SE  $S$  in the building without considering control signaling overhead is

$$S = \sum_{k=1}^{24} S_k \quad (11)$$

where 24 is the number of UEs. The maximal sum SE for 256 QAM is  $S^* = 161.28$  bit/s/Hz, since the rate  $C \left( \text{SINR}_k^{(f)} \right)$  is bounded by 8 bits for 256 QAM.

TABLE I  
SIMULATION PARAMETERS

Carrier frequency	2.1 GHz
Bandwidth	20 MHz
Active bandwidth	18 MHz
Subcarrier spacing	15 kHz
Number of subcarriers	1200
Number of PRBs	100
Antenna spacing	$\lambda_L/2$
Indoor wall penetration loss	12 dB
Per-BS power constraint $P_i$	$26 \text{ dBm} - 10 \log_{10}(N_{\text{BS}})$
Noise level $\sigma_N^2$	-125.1 dBm
Modulation scheme	256 QAM
Number of UEs $K$	24
Number of drops	300
Number of channel realizations per drop	10

## VI. SUM SPECTRAL EFFICIENCY

We first analyze the average sum SE  $S$ . We do not show the 5%-tile sum SE and the 95%-tile sum SE as they follow the same trends. For the *single central BS* deployment there is only one BS, hence the curves for local precoding, LS-MIMO and network MIMO are equal.

Consider the sum SE achieved with network MIMO (solid curves) in Figure 2. The deployments perform poorly for the fully loaded MIMO system with  $M = 24$  BS antennas. The sum SE improves significantly when few antennas are added. Adding more antennas increases the sum SE, but the gain per additional antenna decreases. A ratio of twice as many BS antennas as UEs seems to be a good trade-off between achieved sum SE and number of BS antennas. As expected, the distributed deployments outperform the *single central BS* deployment, except for the *outdoor BSs* deployment which performs poorly with all transmission schemes.

Next consider the sum SE achieved with LS-MIMO (dashed curves) in Figure 2. Recall that for LS-MIMO at least  $M = N_{\text{BS}}K$  total BS antennas are required. Similar to network MIMO, adding more antennas increases the sum SE, and the gain with each additional antenna decreases. Since LS-MIMO does not require a backhaul one can trade off the costs of a backhaul with the number  $M$  of BS antennas to achieve the sum SE of network MIMO with LS-MIMO.

Local precoding is non-cooperative and performs poorly due to interference (dotted curves), see Figure 3. For all deployments the sum SE improves little when adding antennas. However, it may be beneficial to distribute BS antennas even without cooperation. For example, the *two indoor BSs* deployment with local precoding outperforms the *single central BS* deployment. Local precoding outperforms network MIMO for small  $M$  when more UEs are served by a BS than the BS can serve with local precoding and only the best UEs are scheduled.

In conclusion, the SE increases with the number of BS antennas for all deployments and all transmission schemes until it is limited by the maximal SE of the modulation. Cooperation between indoor BSs provides large gains, while cooperation between outdoor BSs, or indoor and outdoor BSs provides smaller gains. Network MIMO performs best, but CS/CB is

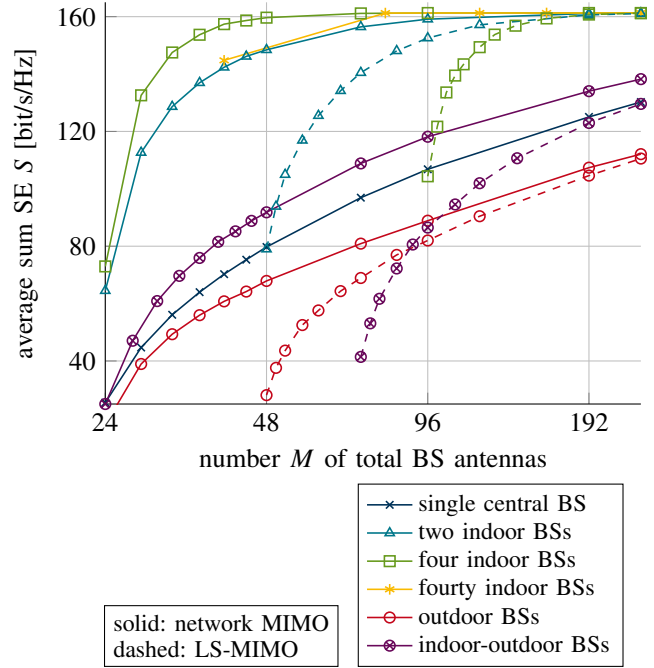


Fig. 2. Average sum SEs with network MIMO and LS-MIMO for 256 QAM and mercury/water-filling.

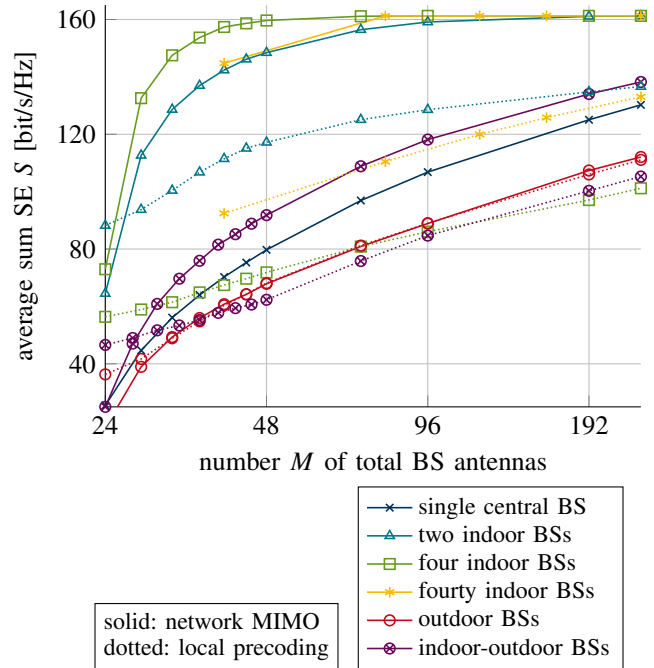


Fig. 3. Average sum SEs with network MIMO and local precoding for 256 QAM and mercury/water-filling.

an interesting alternative as the backhaul requirements are reduced. The placement of BSs is important to overcome wall penetration losses and to control interference.

## VII. AVERAGE SNR MAPS

In this section, we show why the deployments with only one or no indoor BS perform poorly as compared to the distributed indoor BSs deployments. We analyze the SNR achieved when

only a single UE is served at different positions within the office building. The BSs use network MIMO under per-BS power constraints.<sup>1</sup> We distribute the per-BS transmit power equally among the subcarriers. The SNR achieved when a single UE is served is an upper bound to the SNR when more UEs are served with ZFBF or any other linear precoding scheme, as serving more UEs only reduces the degrees-of-freedom.

Figure 4 shows the SNRs averaged over 300 channel realizations for each sampled position. The *single central BS* deployment achieves low SNR in many rooms, especially those close to the outside wall. This is due to the wall penetration loss. The *outdoor BSs* deployment and the *indoor-outdoor BSs* deployment achieve low SNR in inner rooms and in the corridors. The other deployments achieve high SNR in all rooms. We conclude that the lower SEs of the deployments with only one or no indoor BS are at least partly due to the large wall penetration loss and the building penetration loss. A deployment with few well-placed BSs suffices to provide good service throughout the building.

### VIII. COMPARISON TO CAPACITY UPPER BOUND

Massive MIMO lets simple transmission schemes approach capacity with an increasing number of BS antennas. In the following, we analyze this statement for the network MIMO transmission scheme. We upper bound the capacity of a deployment by the capacity of a BC under a total power constraint. We allow all BSs of a deployment to cooperate and to act as one BS with distributed antennas, and relax the per-BS power constraint to a total-power constraint. Note that for the *single central BS* deployment the upper bound is tight, as the capacity of a BC is achieved by non-linear DPC [30], [31], [32], [33]. We find the optimal transmission policy with the algorithms in [34] treating the OFDM subcarriers as virtual antennas. We compare capacity to the SEs achieved with Gaussian modulation, since 256 QAM limits SE, while Gaussian modulation allows to approach the capacity upper bound.

Figure 5 shows the capacity upper bounds, and the average sum SEs achieved with Gaussian modulation and network MIMO under per-BS power constraints and under a total power constraint. The general trends are similar to Figure 2 and Figure 3, but the SEs increase without bound with the number of BS antennas. For few BS antennas, the gap between the capacity upper bound and network MIMO is large, but the gap could be reduced by more advanced scheduling. The channels harden for more BS antennas: It becomes optimal to schedule all UEs on each subcarrier [5], and advanced scheduling strategies provide diminishing gains [13]. With an increasing number of BS antennas, the gap decreases and vanishes completely under a total power constraint, while a gap remains under per-BS power constraints. Determining better capacity upper bounds, and choosing better precoding and power allocation under per-BS power constraints would reduce the gap. In summary, massive MIMO allows simple

transmission schemes to approach capacity with an increasing number of BS antennas in our scenarios.

### IX. FAIRNESS ANALYSIS

Our deployments and transmission schemes should provide a fair service to all UEs as the channels harden. We measure fairness quantitatively with Jain's index [10]

$$J(S_1, S_2, \dots, S_K) = \frac{\left(\sum_{k=1}^K S_k\right)^2}{K \cdot \sum_{k=1}^K S_k^2}. \quad (12)$$

Jain's index is 1 when all UEs achieve the same per-UE SE and is  $1/K$  when only one UE achieves a positive per-UE SE.

Figure 6 shows the simulated fairness indices. For network MIMO and LS-MIMO the *two indoor BSs* deployment, the *four indoor BSs* deployment and the *fourty indoor BSs* deployment approach perfect fairness indices of 1 with an increasing number of BS antennas. This is partly due to all UEs being served with the maximal per-UE SE of 256 QAM. With Gaussian modulation the trends of Jain's fairness index are similar, but no deployment achieves perfect fairness. For local precoding the fairness indices are lower and they do not approach a fairness index of 1 in the range of BS antennas we consider. The *single central BS* deployment, the *outdoor BSs* deployment and the *indoor-outdoor BSs* deployment do not approach a fairness index of 1 with any transmission scheme in the range of BS antennas, but the index increases with the number  $M$  of BS antennas.

We conclude that fairness increases with the number of BS antennas, with the level of cooperation between BSs, and with the distribution of BS antennas (given some cooperation between BSs). Note that one can increase fairness by making it an objective while scheduling and allocating power.

### X. NOISY CHANNEL ESTIMATION

So far we analyzed performance with perfect CSI. However, perfect CSI is usually not available. We analyze the effect of estimation errors on the average SE. We denote the channel coefficient with estimation error from the  $m$ -th antenna of the  $i$ -th BS to the  $k$ -th UE at subcarrier  $f$  as

$$\hat{h}_{i,k,m}^{(f)} = h_{i,k,m}^{(f)} + e_{i,k,m}^{(f)} \quad (13)$$

where  $h_{i,k,m}^{(f)}$  is the channel coefficient without error and  $e_{i,k,m}^{(f)}$  is the estimation error. We model the estimation errors as independent and zero-mean proper complex Gaussian random variables. The estimation error of the channel between the  $i$ -th BS and the  $k$ -th UE is normalized such that its variance scales with the mean channel coefficient squared

$$\mathbb{E} \left[ \left| e_{i,k,m}^{(f)} \right|^2 \right] = \mathbb{E} \left[ \left| h_{i,k,m}^{(f)} \right|^2 \right] \sigma_E^2 \quad (14)$$

where  $\sigma_E^2$  is the normalized mean squared error (NMSE), and the expectation is over the BS antennas and the subcarriers. This channel estimation error occurs, e.g., for channel prediction [11]. We determine the precoders based on the channel estimation with error. For these precoders, intra-cell interference occurs due to the estimation error.

<sup>1</sup>For a single served UE, ZFBF coincides with maximum ratio transmission.

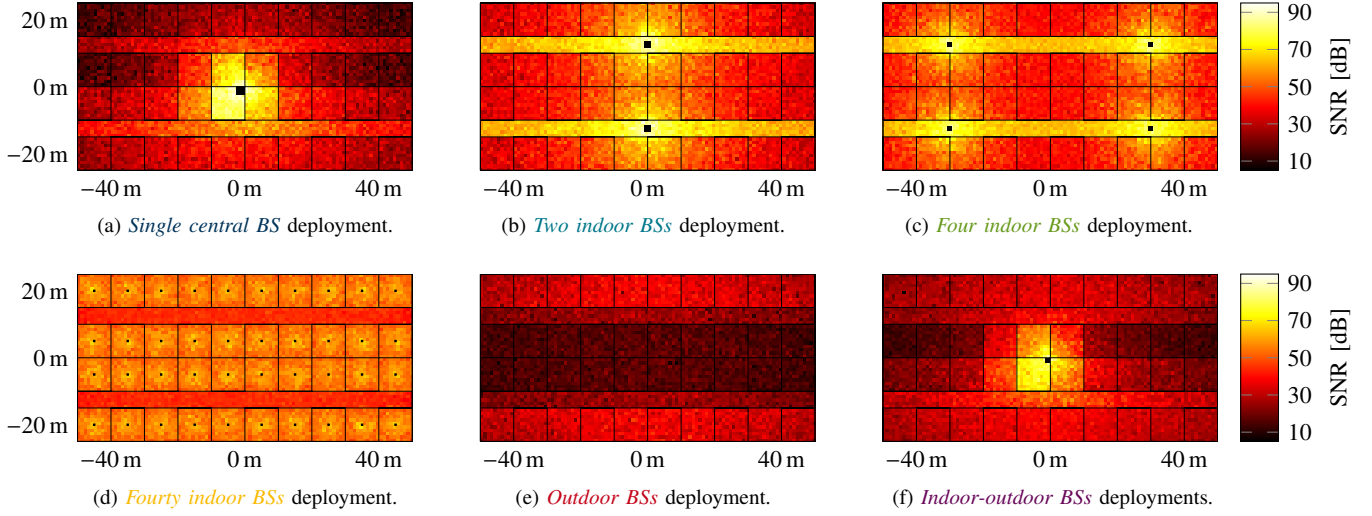


Fig. 4. Average SNR achieved at a single served UE for different positions with 48 transmit antennas (with 40 transmit antennas for the *fourty indoor BSs* deployment).

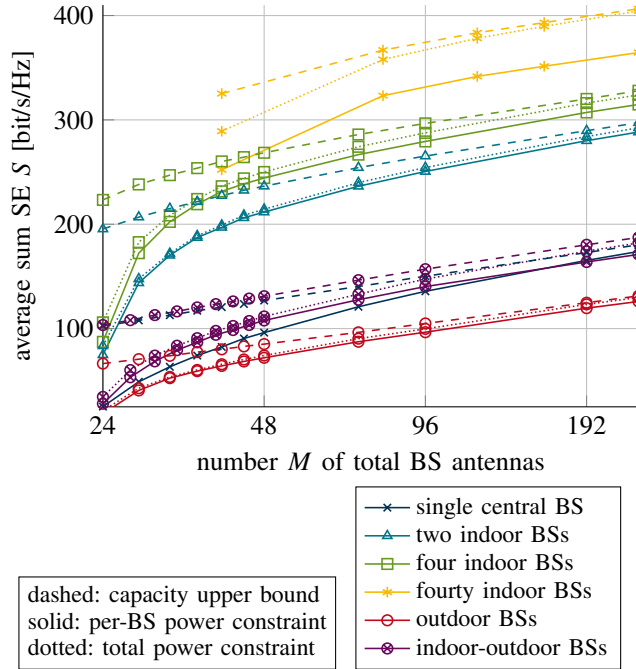


Fig. 5. Average sum SEs of network MIMO for Gaussian modulation.

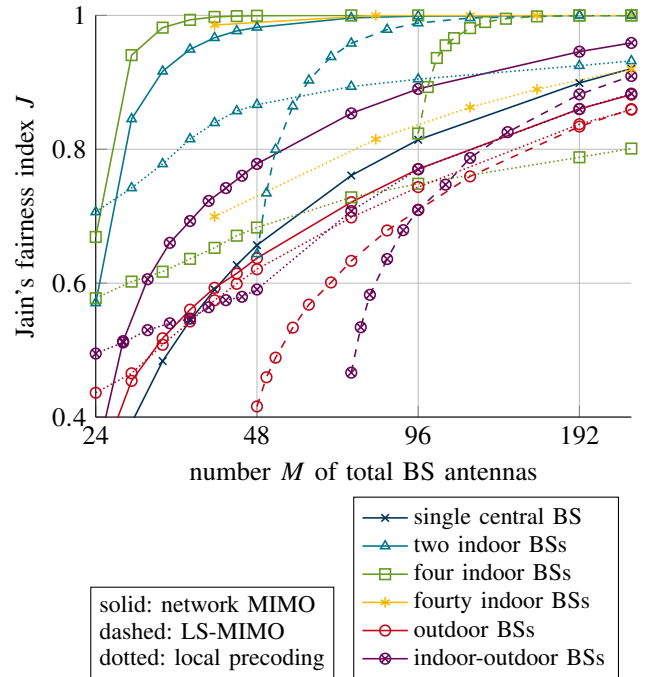


Fig. 6. Jain's fairness index for 256 QAM and mercury/water-filling.

Figure 7 shows the average SEs versus NMSE for 48 total transmit antennas, except for the *fourty indoor BSs* deployment where we deploy only 40 total BS antennas. With network MIMO the performance of all deployments severely degrades with increasing NMSE. The SEs of local precoding are unaffected by low NMSE and degrade for high NMSE only. Inter-cell interference is always present for local precoding and dominates over the interference caused by channel estimation errors for most of the NMSE range. Hence the power allocation of local precoding is more robust to interference and local precoding outperforms network MIMO for a NMSE higher than  $-30$  dB to  $-20$  dB. However, the

performance of network MIMO with estimation errors can be improved, e.g., by making the power allocation more robust to the additional interference caused by estimation errors [35].

For more BS antennas the trends and performance differences are similar. We conclude that all deployments suffer from channel estimation noise, while some deployments are more sensitive. Good channel estimation is crucial to obtain the massive MIMO and network MIMO benefits. However, more robust precoding techniques and power allocation schemes could improve performance in the presence of prediction errors.

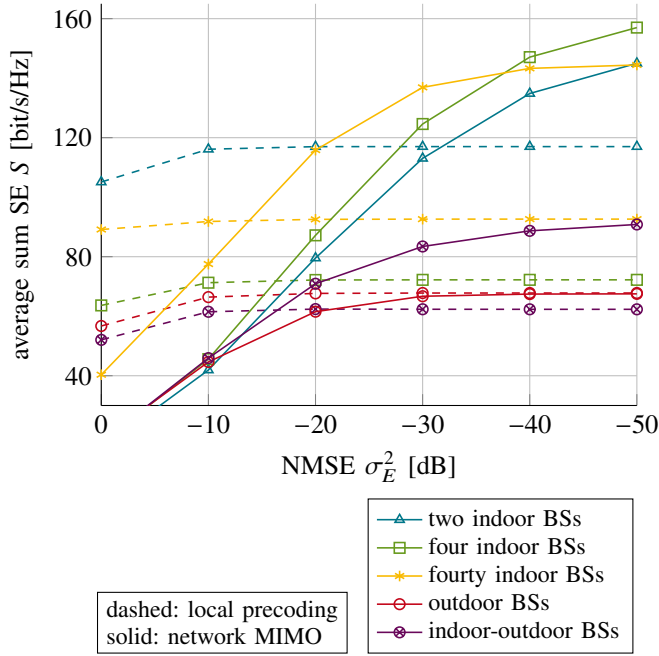


Fig. 7. Average SE with 48 total BS antennas (with 40 total BS antennas for the *four indoor BSs* deployment) for a zero-mean Gaussian distributed channel estimation error.

## XI. CONCLUSIONS

We compared the performance of six different deployments and different levels of cooperation in the 3GGP indoor office scenario. Cooperation between BSs provides gains as compared to no cooperation, which become larger as the level of cooperation increases. The same performance as a single massive MIMO BS is achieved by distributed BSs with cooperation and fewer antennas. The costs of antenna elements can be traded off with the costs for backhaul capability to achieve the same performance. A ratio of twice as many BS antennas as served UEs offers many of the massive MIMO benefits. User fairness and SE close to capacity are achieved with a simple transmission scheme. Accurate channel estimation is necessary to obtain the massive MIMO and cooperation benefits.

A SE of 100 bit/s/Hz without considering overhead is achievable with 192 antennas using local precoding, and less than 28 antennas using two indoor BSs with network MIMO. Considering an overhead of 50%, the required bandwidth to achieve the goals of the METIS project [1] is:

- For the TC1 virtual reality office:

$$\frac{0.1 \text{ Gbit/s/m}^2 \cdot 5000 \text{ m}^2}{50 \text{ bit/s/Hz}} = 10 \text{ GHz}. \quad (15)$$

More UE antennas, more base stations, or larger QAM constellations could reduce the required bandwidth.

- For the TC2 dense urban information society:

$$\frac{0.7 \text{ Mbit/s/m}^2 \cdot 5000 \text{ m}^2}{50 \text{ bit/s/Hz}} = 70 \text{ MHz}. \quad (16)$$

This performance is achievable with single antenna UEs, few BSs, and 256 QAM within a reasonable bandwidth.

## ACKNOWLEDGMENT

S. Dierks and G. Kramer were supported in part by an Alexander von Humboldt Professorship endowed by the German Federal Ministry of Education and Research.

## REFERENCES

- [1] Mobile and Wireless Communications Enablers for the Twenty-Two Information Society (METIS), "Deliverable D1.1 - scenarios, requirements and KPIs for 5G mobile and wireless system," Tech. Rep., Apr. 2013.
- [2] T. Marzetta, "Noncooperative cellular wireless with unlimited numbers of base station antennas," *IEEE Trans. Wireless Commun.*, vol. 9, no. 11, pp. 3590–3600, Nov. 2010.
- [3] E. Larsson, O. Edfors, F. Tufvesson, and T. Marzetta, "Massive MIMO for next generation wireless systems," *IEEE Commun. Mag.*, vol. 52, no. 2, pp. 186–195, Feb. 2014.
- [4] F. Rusek, D. Persson, B. K. Lau, E. G. Larsson, T. L. Marzetta, O. Edfors, and F. Tufvesson, "Scaling up MIMO: Opportunities and challenges with very large arrays," *IEEE Signal Process. Mag.*, vol. 30, no. 1, pp. 40–60, Jan. 2013.
- [5] E. Björnson, E. G. Larsson, and T. L. Marzetta, "Massive MIMO: Ten myths and one critical question," *IEEE Commun. Mag.*, vol. 54, no. 2, pp. 114–123, Feb. 2016.
- [6] E. Björnson, M. Bengtsson, and B. Ottersten, "Optimal multiuser transmit beamforming: A difficult problem with a simple solution structure [lecture notes]," *IEEE Signal Process. Mag.*, vol. 31, no. 4, pp. 142–148, Jul. 2014.
- [7] M. Costa, "Writing on dirty paper," *IEEE Trans. Inf. Theory*, vol. 29, no. 3, pp. 439–441, May 1983.
- [8] J. Zhang and G. de la Roche, Eds., *Femtocells: Technologies and Deployment*. John Wiley & Sons, 2013.
- [9] 3GPP, "TR36.814 - further advancements for E-UTRA physical layer aspects," Tech. Rep. v9.0.0, Mar. 2010.
- [10] R. Jain, D.-M. Chiu, and W. R. Hawe, "A quantitative measure of fairness and discrimination for resource allocation in shared computer systems," DEC Research Report, Tech. Rep. 301, 1984.
- [11] S. Dierks, M. Amin, W. Zirwas, M. Haardt, and B. Panzner, "The benefit of cooperation in the context of massive MIMO," in *18th Int. OFDM Workshop (InOWoS)*, Aug. 2014, pp. 1–8.
- [12] B. Panzner, W. Zirwas, S. Dierks, M. Lauridsen, P. Mogensen, K. Pajukoski, and D. Miao, "Deployment and implementation strategies for massive MIMO in 5G," in *IEEE Global Telecommun. Conf. (Globecom) Workshop Massive MIMO*, Dec. 2014.
- [13] S. Dierks, W. Zirwas, M. Jäger, B. Panzner, and G. Kramer, "MIMO and massive MIMO - analysis for a local area scenario," in *23rd European Signal Processing Conf. (EUSIPCO)*, Sep. 2015, pp. 2496–2500.
- [14] A. Lozano, A. M. Tulino, and S. Verdú, "Optimum power allocation for parallel Gaussian channels with arbitrary input distributions," *IEEE Trans. Inf. Theory*, vol. 52, no. 7, pp. 3033–3051, Jul. 2006.
- [15] IST, "D1.1.2 - WINNER II channel models," Tech. Rep. v1.2, 2008.
- [16] G. Boudreau, J. Panicker, N. Guo, R. Chang, N. Wang, and S. Vrzic, "Interference coordination and cancellation for 4G networks," *IEEE Commun. Mag.*, vol. 47, no. 4, pp. 74–81, Apr. 2009.
- [17] D. Lee, H. Seo, B. Clerckx, E. Hardouin, D. Mazzaresse, S. Nagata, and K. Sayana, "Coordinated multipoint transmission and reception in LTE-advanced: Deployment scenarios and operational challenges," *IEEE Commun. Mag.*, vol. 50, no. 2, pp. 148–155, Feb. 2012.
- [18] E. Björnson and E. Jorswieck, "Optimal resource allocation in coordinated multi-cell systems," *Foundations and Trends in Communications and Information Theory*, vol. 9, no. 2-3, pp. 113–381, 2013. [Online]. Available: <http://dx.doi.org/10.1561/01000000069>
- [19] A. Wiesel, Y. Eldar, and S. Shamai, "Zero-forcing precoding and generalized inverses," *IEEE Trans. Signal Proc.*, vol. 56, no. 9, pp. 4409–4418, Sep. 2008.
- [20] X. Zhang and J. Lee, "Low complexity MIMO scheduling with channel decomposition using capacity upperbound," *IEEE Trans. Commun.*, vol. 56, no. 6, pp. 871–876, Jun. 2008.
- [21] D. Gesbert, S. Hanly, H. Huang, S. S. Shitz, O. Simeone, and W. Yu, "Multi-cell MIMO cooperative networks: A new look at interference," *IEEE J. Sel. Areas Commun.*, vol. 28, no. 9, pp. 1380–1408, Dec. 2010.
- [22] K. Hosseini, W. Yu, and R. S. Adve, "Large-scale MIMO versus network MIMO for multicell interference mitigation," *IEEE J. Sel. Topics Signal Process.*, vol. 8, no. 5, pp. 930–941, Oct. 2014.



- [23] R. Zhang, "Cooperative multi-cell block diagonalization with per-base-station power constraints," *IEEE J. Sel. Areas Commun.*, vol. 28, no. 9, pp. 1435–1445, Dec. 2010.
- [24] S. Shi, M. Schubert, N. Vucic, and H. Boche, "MMSE optimization with per-base-station power constraints for network MIMO systems," in *IEEE Int. Conf. Communications (ICC)*, May 2008, pp. 4106–4110.
- [25] H. Zhang and H. Dai, "On the capacity of distributed MIMO systems," in *38th Conf. Inform. Sciences and Systems (CISS)*, 2004.
- [26] A. Forenza, S. Perlman, F. Saibi, M. D. Dio, R. van der Laan, and G. Caire, "Achieving large multiplexing gain in distributed antenna systems via cooperation with pCell technology," in *49th Asilomar Conf. Signals, Systems and Computers (ACSSC)*, Nov. 2015, pp. 286–293.
- [27] S. Jaeckel, L. Raschkowski, K. Börner, L. Thiele, F. Burkhardt, and E. Eberlein, "QuaDRiGa-quasi deterministic radio channel generator, user manual and documentation," Fraunhofer Heinrich Hertz Institute, Tech. Rep. v1.4.1-551, 2016.
- [28] CELTIC, "D5.3: WINNER+ final channel models," Tech. Rep. v1.0, 2010.
- [29] G. Ungerboeck, "Channel coding with multilevel/phase signals," *IEEE Trans. Inf. Theory*, vol. 28, no. 1, pp. 55–67, Jan. 1982.
- [30] G. Caire and S. Shamai, "On the achievable throughput of a multiantenna Gaussian broadcast channel," *IEEE Trans. Inf. Theory*, vol. 49, no. 7, pp. 1691–1706, Jul. 2003.
- [31] P. Viswanath and D. N. C. Tse, "Sum capacity of the vector Gaussian broadcast channel and uplink-downlink duality," *IEEE Trans. Inf. Theory*, vol. 49, no. 8, pp. 1912–1921, Aug. 2003.
- [32] S. Vishwanath, N. Jindal, and A. Goldsmith, "Duality, achievable rates, and sum-rate capacity of Gaussian MIMO broadcast channels," *IEEE Trans. Inf. Theory*, vol. 49, no. 10, pp. 2658–2668, Oct. 2003.
- [33] W. Yu and J. M. Cioffi, "Sum capacity of Gaussian vector broadcast channels," *IEEE Trans. Inf. Theory*, vol. 50, no. 9, pp. 1875–1892, Sep. 2004.
- [34] N. Jindal, W. Rhee, S. Vishwanath, S. Jafar, and A. Goldsmith, "Sum power iterative water-filling for multi-antenna Gaussian broadcast channels," *IEEE Trans. Inf. Theory*, vol. 51, no. 4, pp. 1570–1580, Apr. 2005.
- [35] T. Yoo and A. Goldsmith, "Capacity and power allocation for fading MIMO channels with channel estimation error," *IEEE Trans. Inf. Theory*, vol. 52, no. 5, pp. 2203–2214, May 2006.



physical layer aspects and massive MIMO for 5G. He is currently working at Nokia Networks as Solution Architect for IoT connectivity solutions.



technologies.

**Berthold Panzner** received his M.Sc. degree in telecommunications in 2007 from Linköpings University in Sweden and the PhD degree in electrical engineering from Otto-von-Guericke University Magdeburg in Germany in 2012. He received two best paper awards at the Antenna and Propagation Symposium 2008 and the International Radar Symposium 2012 respectively for his research work on synthetic aperture radar techniques for ground penetrating radar. He joined Nokia Siemens Networks in 2013, where he was involved in the design of

**Wolfgang Zirwas** received his diploma degree in communication technologies in 1987 from Technical University of Munich (TUM). He started his work at the Siemens Munich central research lab for communication technologies with a focus on high frequency and high data rate TDM fiber systems for data rates up to 40 Gbit/s. He participated in several German and EU funded projects like COVERAGE, WINNER, Artist4G, METIS or Fantastic5G. Currently, he is at the end to end Lab of Nokia Bell Labs in Munich investigating 5G mobile radio



**Stefan Dierks** received the B.Sc. and the M.Sc. equivalent Diplom-Ingenieur degree in Electrical Engineering from the Technical University of Munich (TUM) in 2009 and 2011, respectively. Since 2011 he is working towards his doctoral degree at the Chair for Communications Engineering at TUM under the supervision of Prof. Kramer. His research interests include 5G, massive MIMO, cooperative communications, interference alignment, and EIRP.



**Gerhard Kramer** is Alexander von Humboldt Professor and Chair of Communications Engineering at the Technical University of Munich (TUM). He received the B.Sc. and M.Sc. degrees in electrical engineering from the University of Manitoba, Canada, in 1991 and 1992, respectively, and the Dr. sc. techn. degree from the ETH Zurich, Switzerland, in 1998. From 1998 to 2000, he was with Endora Tech AG in Basel, Switzerland, and from 2000 to 2008 he was with the Math Center at Bell Labs in Murray Hill, NJ. He joined the University of Southern California (USC), Los Angeles, CA, as a Professor of Electrical Engineering in 2009. He joined TUM in 2010. Gerhard Kramer's research interests are primarily in information theory and communications theory, with applications to wireless, copper, and optical fiber networks.